Electronic Supplementary Information

Functional Group Dependence of the Acid Catalyzed Ring Opening of Biomass Derived Furan Rings: An Experimental and Theoretical Study

Christopher R. Waidmann,[a] **Aaron W. Pierpont,**[b] **Enrique R. Batista,**[b] **John C. Gordon,***[a]
Richard L. Martin,[b] **L. A. "Pete" Silks***[c]**, Ryan M. West**[d] **and Ruilian Wu**[c]

Chemistry[a], Theoretical[b] and Bioscience Divisions[c], Los Alamos National Laboratory, Los Alamos, New Mexico 87545, USA. Procter & Gamble, West Chester, OH 45069, USA.[d]

Testing Metal Salts as Ring Opening Catalysts

A variety of metal salts were also tested as potential ring opening catalysts in water:methanol mixtures at 80 °C, as summarized in Table 1. Initially, several iron salts were studied. Both $Fe^{III}Cl_3$ and $Fe^{III}(NO_3)_3$ (entries 3 and 4) gave 92% and 94% yields of **2a** after 24 hrs, respectively. Anhydrous $FeCl_3$ and the monohydrate compound $FeCl_3{\cdot}H_2O$ (entry 8) give very similar results. The same yield of **2a** is obtained when catalytic amounts of $FeCl_3$ are used in air or an argon atmosphere with degassed solvent, indicating that oxygen is not required for catalysis. Tests showed that solutions containing $Fe^{III}Cl_3$ and $Fe^{III}(NO_3)_3$ are significantly acidic however: solutions from entries 3 and 4 have a pH of 2, equal to the pH of the HCl solution in entry 2. The low pH of these solutions suggests that these Fe(III) salts act simply as sources of acid (HCl and HNO_3),[1] and not as Lewis acid catalysts. The observed ring opening rates are consistent with generation of approximately one equivalent of acid per iron center, yielding approximately 10 mol % acid. Addition of 10 mol % HCl slightly increased the ring opening yield. In contrast, $Fe^{III}_2(SO_4)_3{\cdot}5H_2O$ yields 64% ring opened product after 24 hours (entry 17).

Other metal salts that were tested did not lower the solution pH dramatically. Of these, $Fe^{II}Cl_2$ is the most effective, giving a 45% yield of **2a**. When heated in air, significant amounts of insoluble iron oxide are observed at the end of the reaction indicating oxidation of the iron center. Oxidation to trivalent iron yields an acidic solution, which is again likely responsible for catalysis. In contrast, only a 4 % yield of **2a** is observed when the reaction is run under an atmosphere of argon in degassed solvent, and no iron oxide formation is observed. $AlCl_3$ proved to be the next most effective, but provides **2a** in only 17% yield. Again, only one product is

---

[1] (a) Nadtochenko, V. A.; Kiwi, J. *Inorg. Chem.* 1998, **37**, 5233-5238. (b) Rodriguez, F.; Moreno, M. *Transition Met. Chem.* 1985, **10**, 108-112.

observed in these reactions. The other salts tested provided little to no yield of **2a**, even after extended reaction times.

Table 1. Yields of **2a** after heating **1a** with 10 mol % catalyst in 1:1 water:methanol mixture at 80 °C for 24 hours.

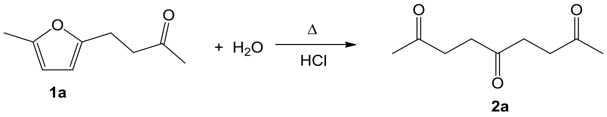

Entry	Catalyst	Yield of **2a**
1	HCl + $FeCl_3$	95%
2	HCl	94%
3	$Fe^{III}Cl_3$	92%
4	$Fe(NO_3)_3·9H_2O$	94%
5	$FeCl_2$	48%
6	$FeCl_2$ (Argon)	4%
7	$AlCl_3$	44%
8	$Lu(OTf)_3$	1%
9	$FeCl_3·H_2O$	93%
10	$FeCl_3$ (Argon)	92%
11	$CuCl_2$	10%
12	Fe_2O_3	0%
13	CuCl	10%
14	$CoCl_2$	0%
15	$CeCl_3$	9%
16	$NiCl_2$	0%
17	$Fe(SO_4)·7H_2O$	14%
18	$Fe_2(SO_4)_3·5H_2O$	64%
19	$MgSO_4$	0%
20	none	0%

Computational Results

S1: Gaussian09 reference

Gaussian 09, Revision **B.01**, Frisch, M. J.; Trucks, G. W.; Schlegel, H. B.; Scuseria, G. E.; Robb, M. A.; Cheeseman, J. R.; Scalmani, G.; Barone, V.; Mennucci, B.; Petersson, G. A.; Nakatsuji, H.; Caricato, M.; Li, X.; Hratchian, H. P.; Izmaylov, A. F.; Bloino, J.; Zheng, G.; Sonnenberg, J. L.; Hada, M.; Ehara, M.; Toyota, K.; Fukuda, R.; Hasegawa, J.; Ishida, M.; Nakajima, T.; Honda, Y.; Kitao, O.; Nakai, H.; Vreven, T.; Montgomery, Jr., J. A.; Peralta, J. E.; Ogliaro, F.; Bearpark, M.; Heyd, J. J.; Brothers, E.; Kudin, K. N.; Staroverov, V. N.; Kobayashi, R.; Normand, J.; Raghavachari, K.; Rendell, A.; Burant, J. C.; Iyengar, S. S.; Tomasi, J.; Cossi, M.; Rega, N.; Millam, N. J.; Klene, M.; Knox, J. E.; Cross, J. B.; Bakken, V.; Adamo, C.; Jaramillo, J.; Gomperts, R.; Stratmann, R. E.; Yazyev, O.; Austin, A. J.; Cammi, R.; Pomelli, C.; Ochterski, J. W.; Martin, R. L.; Morokuma, K.; Zakrzewski, V. G.; Voth, G. A.; Salvador, P.; Dannenberg, J. J.; Dapprich, S.; Daniels, A. D.; Farkas, Ö.; Foresman, J. B.; Ortiz, J. V.; Cioslowski, J.; Fox, D. J. Gaussian, Inc., Wallingford CT, 2009.

S2: Geometry changes in 1b on protonation

C5 protonation

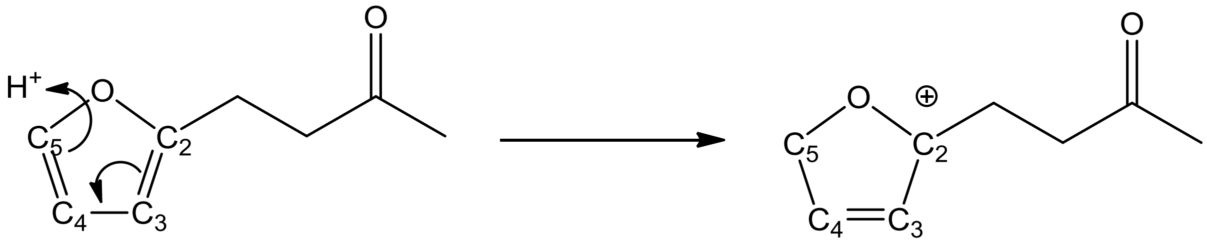

C2-O:	1.37 Å	1.30 Å
C2-C3:	1.36 Å	1.43 Å
C3-C4:	1.44 Å	1.35 Å
C4-C5:	1.36 Å	1.47 Å
C5-O:	1.37 Å	1.46 Å

C2 protonation

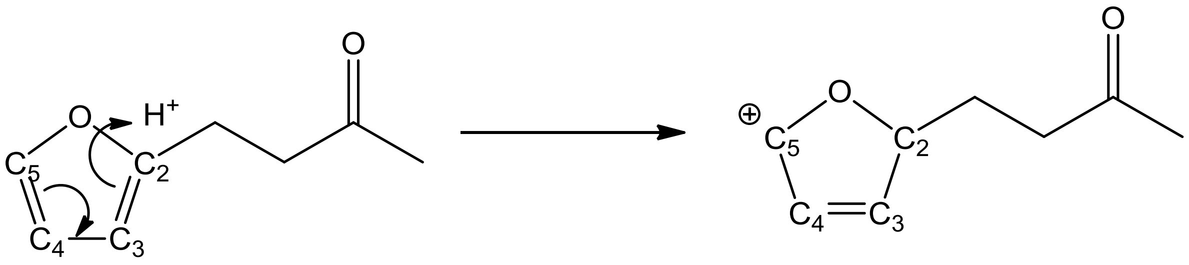

C2-O:	1.37	1.48
C2-C3:	1.36	1.48
C3-C4:	1.44	1.36
C4-C5:	1.36	1.42
C5-O:	1.37	1.28

* CPCM/CBS-QB3 optimized geometries. Bond lengths in Å.

S3: CPCM/B3LYP/6-311+G(d) Optimized geometries of 2b*, 2c, and 2e

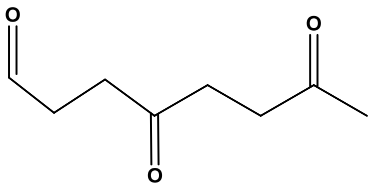

2b*

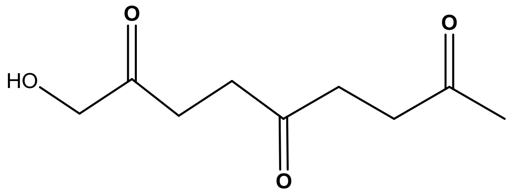

2c

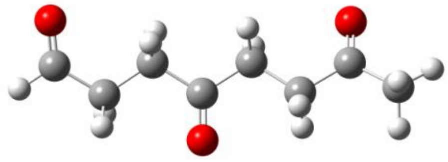

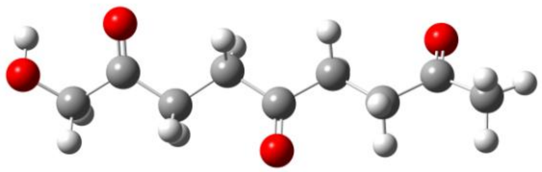

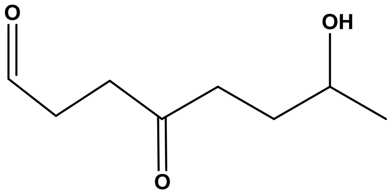

2e

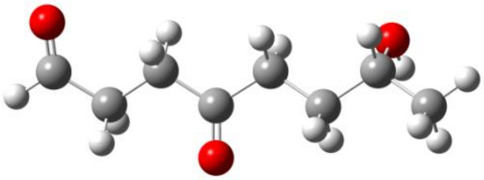

S4: Proton migration during geometry optimization

1c

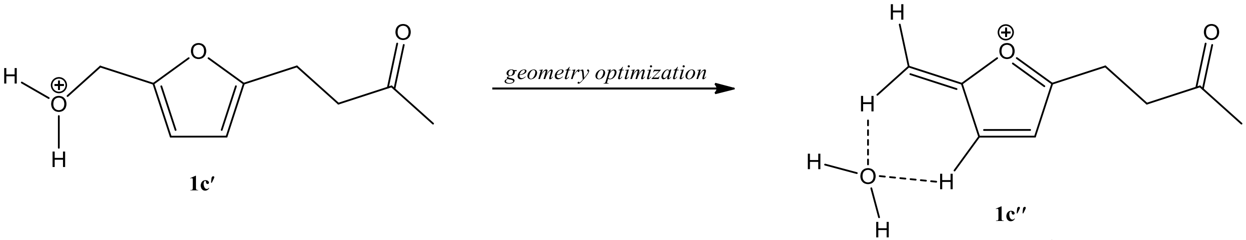

1c′

1c′′
(CBS-QB3)

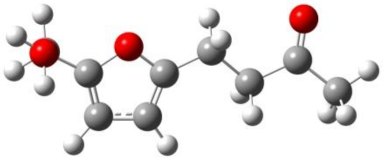

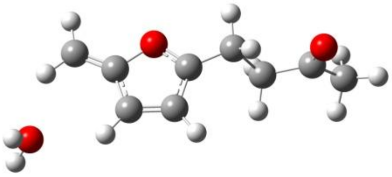

Electronic Supplementary Information

<u>3a</u>

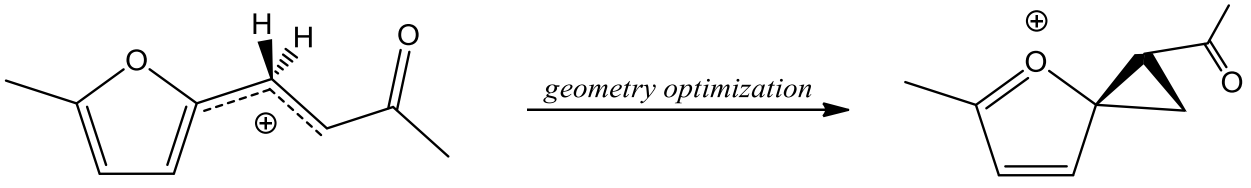

3a′

(CBS-QB3)

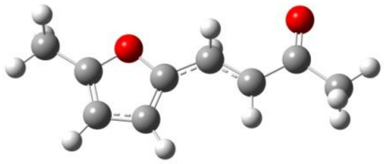

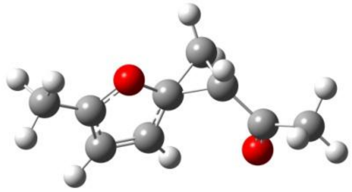

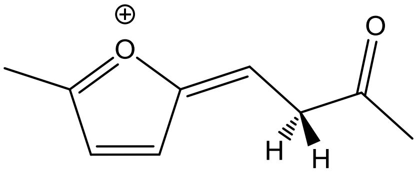

(CPCM/ CBS-QB3)

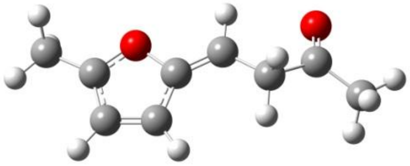

Electronic Supplementary Information

3b

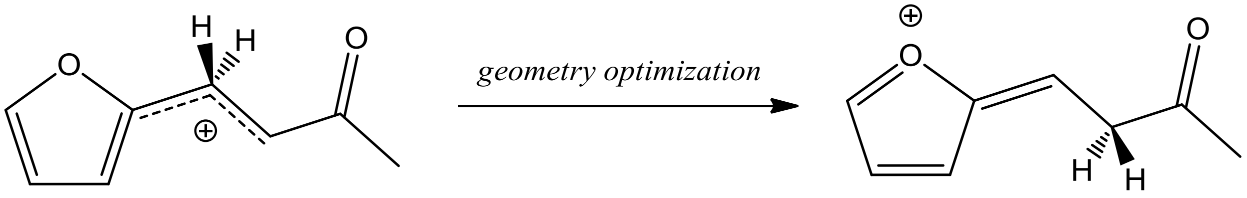

(CBS and CPCM/CBS-QB3)

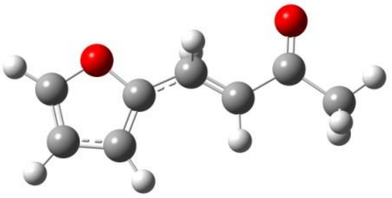

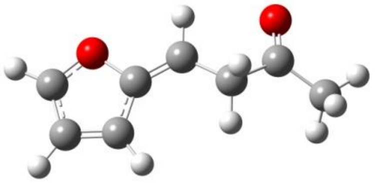

3c

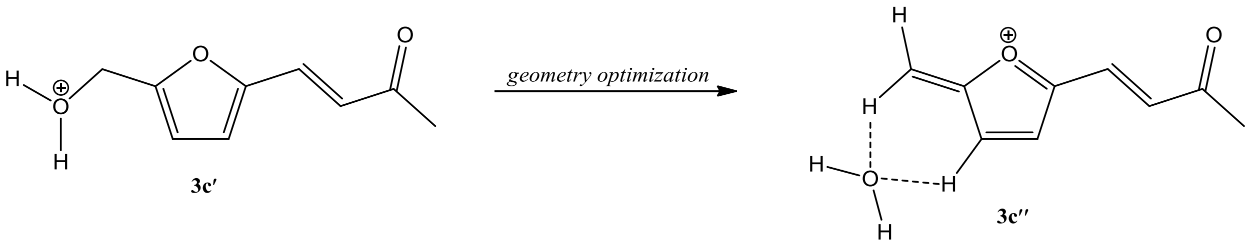

3c′

3c″
(CBS-QB3)

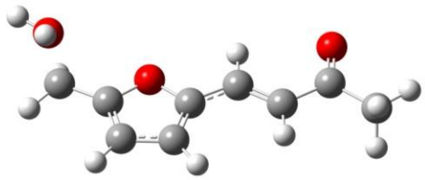

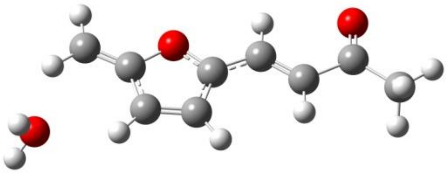

Electronic Supplementary Information

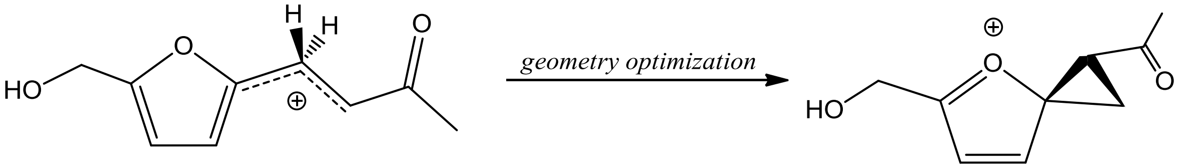

(CBS-QB3)

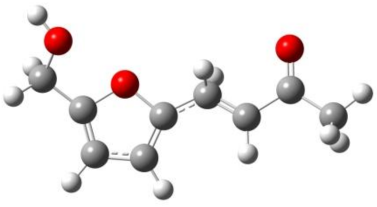

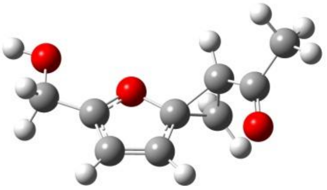

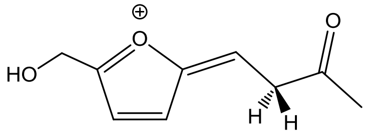

(CPCM/CBS-QB3)

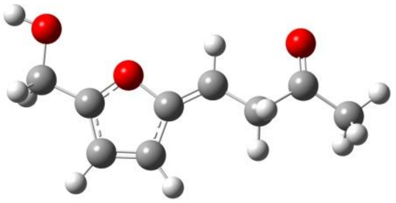

S5: Stabilization of protonated CH_2OH in 1c, 1d, 1e, and 3c with an explicit H_2O molecule

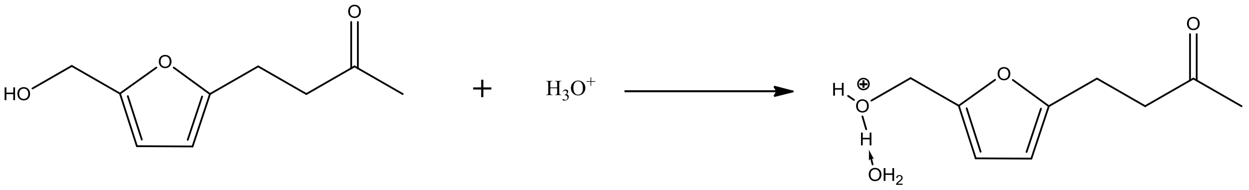

1c

1c-H_3O^+

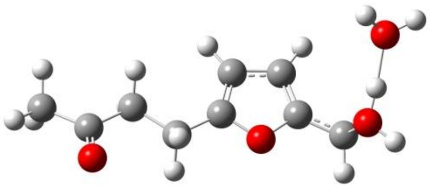

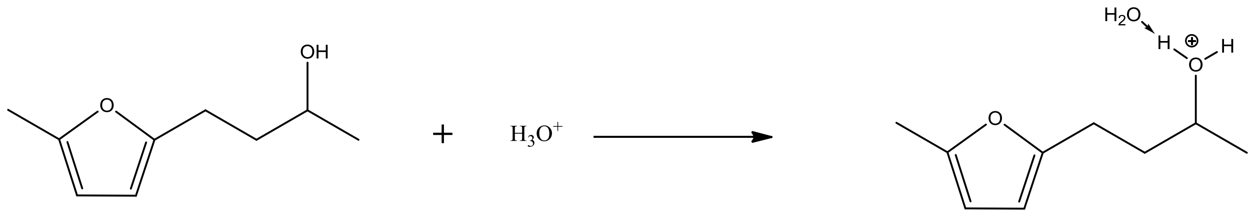

1d

1d-H_3O^+

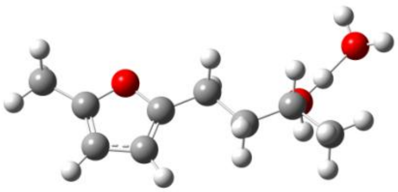

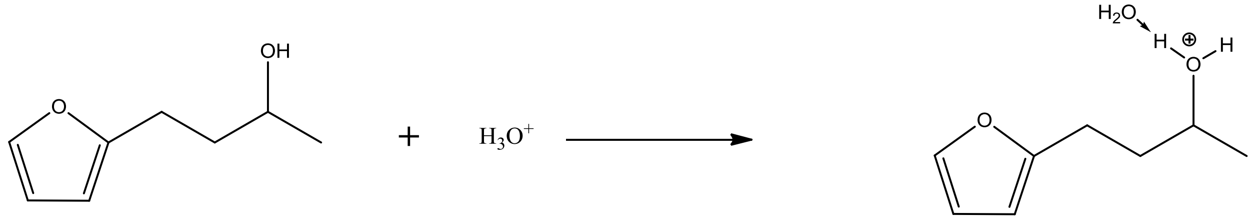

1e

1e-H_3O^+

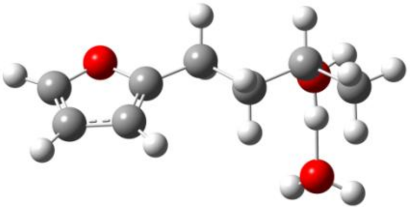

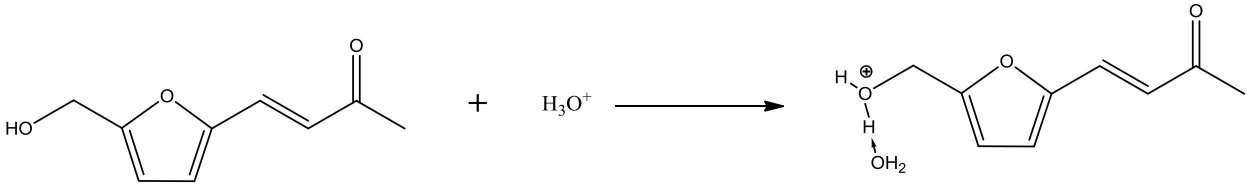

3c

3c-H_3O^+

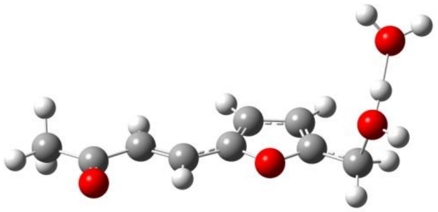

S6: Geometries of ketone-protonated 1a-1c and 3a-3c with an explicit H_2O molecule

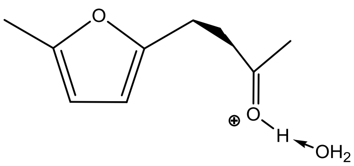

1a-COH$^+$-H_2O

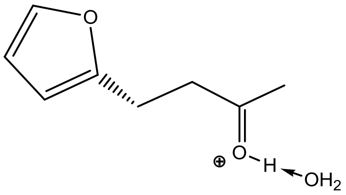

1b-COH$^+$-H_2O

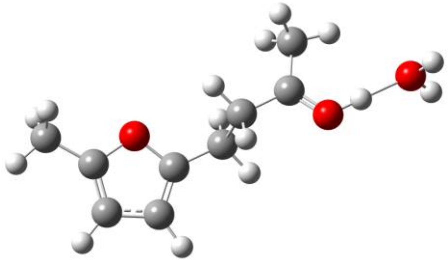

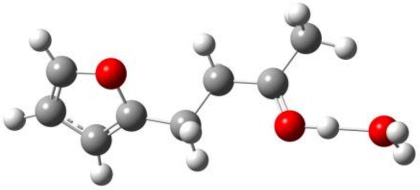

Electronic Supplementary Information

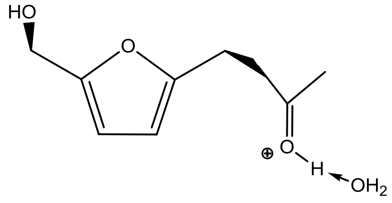

1c-COH$^+$-H$_2$O

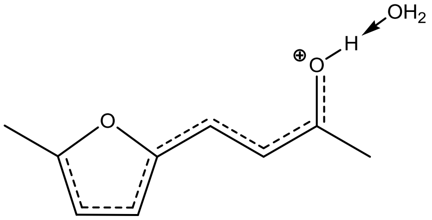

3a-COH$^+$-H$_2$O

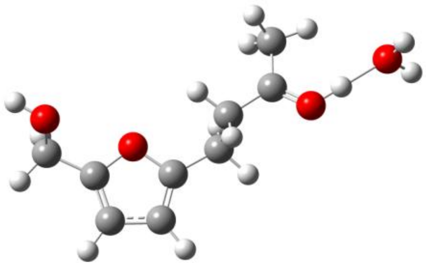

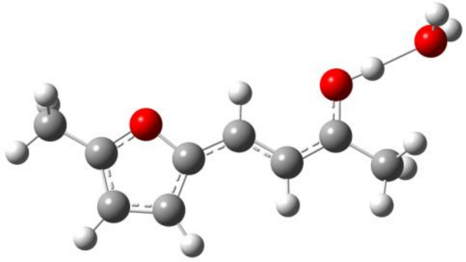

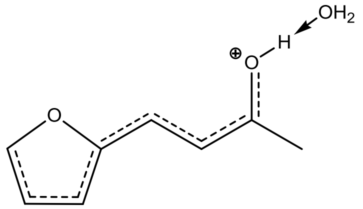

3b-COH$^+$-H$_2$O

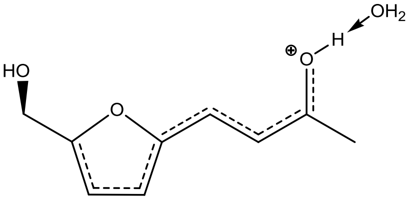

3c-COH$^+$-H$_2$O

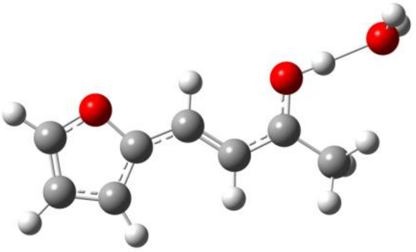

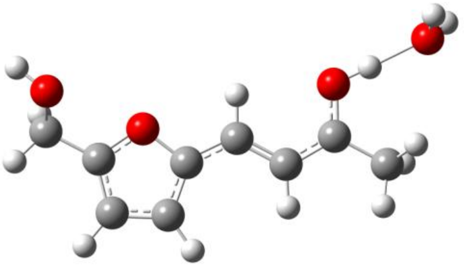

Modified thermodynamic cycle for including an explicit H$_2$O molecule

$$\begin{tikzcd}
\mathbf{1c(g)} \arrow[d, "\Delta G_{solv}(1c)"'] & + & \mathbf{H_3O^+(g)} \arrow[r, "\Delta G_g - 1.89"] \arrow[d, "\Delta G_{solv}(H_3O^+)"] & \mathbf{1c\text{-}H_3O^+(g)} \arrow[d, "\Delta G_{solv}(1c\text{-}H_3O^+)"] \\
\mathbf{1c(aq)} & + & \mathbf{H_3O^+(aq)} \arrow[r, "\Delta G_{aq}"] & \mathbf{1c\text{-}H_3O^+(aq)}
\end{tikzcd}$$

The value 1.89 kcal/mol is added to the gas phase protonation free energy to convert from an ideal gas standard state of 1 atm (24.46 L/mol) to a standard state of 1 M:

$$\Delta G(\mathrm{atm} \rightarrow \mathrm{M}) = RT\ln(24.46) = 1.89 \text{ kcal/mol at } 298.15 \text{ K}$$

S7: Solvation free energies (CPCM/B3LYP/6-311+G(d)) of furans and ring-opened products

Furans	ΔG_{solv} [a]	Ring-opened products	ΔG_{solv}
1a	-8.17	**2a**	-12.69
1b	-6.50	**2b***	-9.82
1c	-15.38	**2c**	-17.58
1d	-5.63	**2d**	-9.99
1e	-5.60	**2e**	-10.17
3a	-9.70	**4a**	-13.07
3b	-6.28	**4b**	-10.14
3c	-17.79	**4c**	-12.32

[a] Free energies in kcal/mol

S8: Effect of B3LYP vs. HF solvation energies on pK_as

$$\Delta pK_a = (pK_a(\text{CPCM/B3LYP/6-311+G(d)}) - (pK_a(\text{CPCM/HF/6-31G(d)})$$

1a

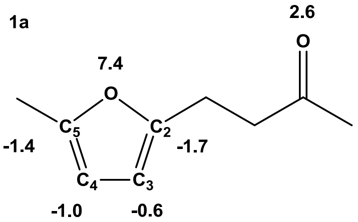

1b

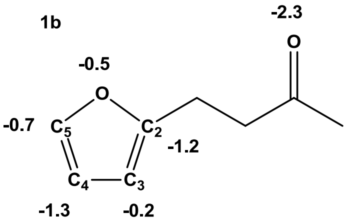

1c

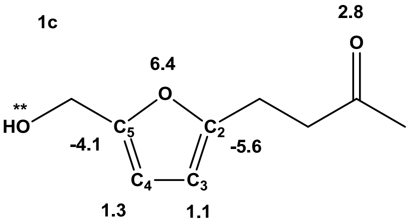

1d

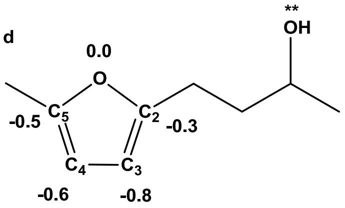

1e

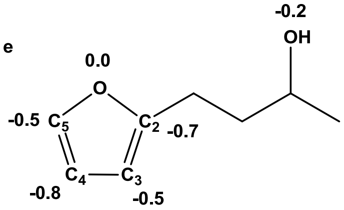

3a

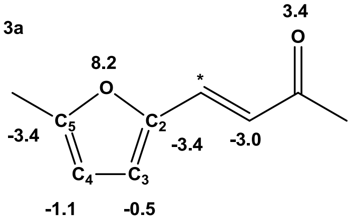

3b

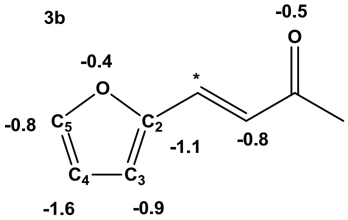

3c

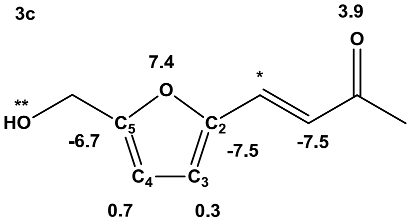

* Proton migrates across double bond during optimization

** Adding an explicit H_2O gave different gas phase and solution geometries for B3LYP

Electronic Supplementary Material (ESI) for Catalysis Science & Technology

Electronic Supplementary Information

CPCM/B3LYP/6-311+G(d) pK_as

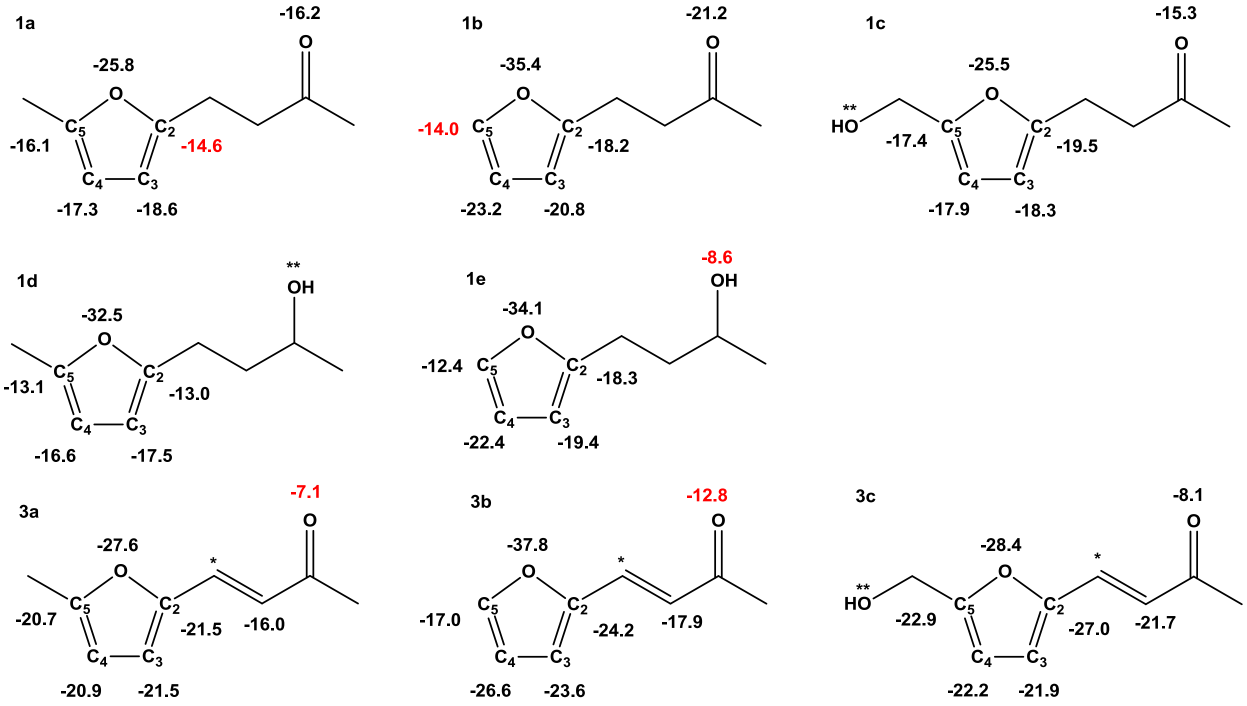

* Proton migrates across double bond during optimization

** Adding an explicit H_2O gave different gas phase and solution geometries for B3LYP

S9: Use of CPCM solvation free energies for p*K*a s of protonated carbonyls and hydroxyls with explicit water molecule

CPCM/HF/6-31G(d) p*K*a s

1a

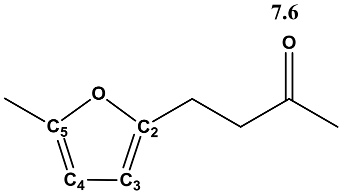

1b

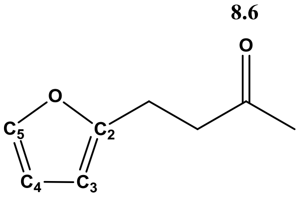

1c

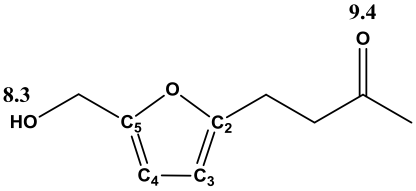

1d

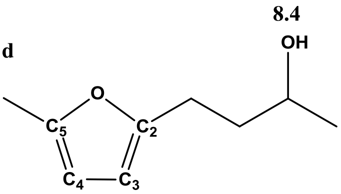

1e

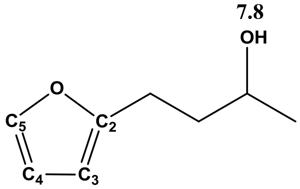

3a

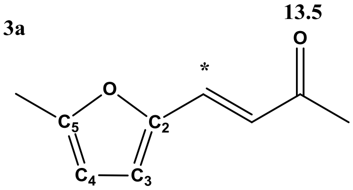

3b

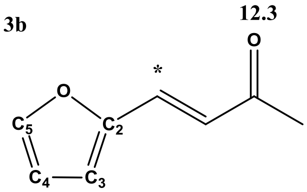

3c

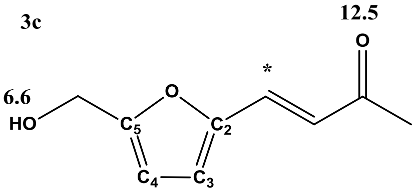

* Proton migrates across double bond during optimization